Since January 2020 Elsevier has created a COVID-19 resource centre with free information in English and Mandarin on the novel coronavirus COVID-19. The COVID-19 resource centre is hosted on Elsevier Connect, the company's public news and information website.

Elsevier hereby grants permission to make all its COVID-19-related research that is available on the COVID-19 resource centre - including this research content - immediately available in PubMed Central and other publicly funded repositories, such as the WHO COVID database with rights for unrestricted research re-use and analyses in any form or by any means with acknowledgement of the original source. These permissions are granted for free by Elsevier for as long as the COVID-19 resource centre remains active.

Decision Analytics Journal 6 (2023) 100156

Contents lists available at ScienceDirect

Decision Analytics Journal

journal homepage: www.elsevier.com/locate/dajour

A new fractional mathematical model to study the impact of vaccination on COVID-19 outbreaks

Shyamsunder [a], S. Bhatter [a], K. Jangid [b], A. Abidemi [c,*], K.M. Owolabi [c], S.D. Purohit [d]

[a] Department of Mathematics, Malaviya National Institute of Technology Jaipur, India
[b] Department of Mathematics, Central University of Rajasthan, Ajmer, India
[c] Department of Mathematical Sciences, Federal University of Technology, Akure, Ondo State, Nigeria
[d] Department of HEAS (Mathematics), Rajasthan Technical University, Kota, India

ARTICLE INFO

MSC:
26A33
34A08
37N25
65P99
92D30

Keywords:
Corona virus
Caputo fractional derivative
Laplace transform
Existence and stability
Numerical simulations

ABSTRACT

This study proposes a new fractional mathematical model to study the impact of vaccination on COVID-19 outbreaks by categorizing infected people into non-vaccinated, first dose-vaccinated, and second dose-vaccinated groups and exploring the transmission dynamics of the disease outbreaks. We present a non-linear integer order mathematical model of COVID-19 dynamics and modify it by introducing Caputo fractional derivative operator. We start by proving the good state of the model and then calculating its reproduction number. The Caputo fractional-order model is discretized by applying a reliable numerical technique. The model is proven to be stable. The classical model is fitted to the corresponding cumulative number of daily reported cases during the vaccination regime in India between 01 August 2021 and 21 July 2022. We explore the sensitivities of the reproduction number with respect to the model parameters. It is shown that the effective transmission rate and the recovery rate of unvaccinated infected individuals are the most sensitive parameters that drive the transmission dynamics of the pandemic in the population. Numerical simulations are used to demonstrate the applicability of the proposed fractional mathematical model via the memory index at different values of $0.7, 0.8, 0.9$ and 1. We discuss the epidemiological significance of the findings and provide perspectives on future health policy tendencies. For instance, efforts targeting a decrease in the transmission rate and an increase in the recovery rate of non-vaccinated infected individuals are required to ensure virus-free population. This can be achieved if the population strictly adhere to precautionary measures, and prompt and adequate treatment is provided for non-vaccinated infectious individuals. Also, given the ongoing community spread of COVID-19 in India and almost the pandemic-affected countries worldwide, the need to scale up the effort of mass vaccination policy cannot be overemphasized in order to reduce the number of unvaccinated infections with a view to halting the transmission dynamics of the disease in the population.

1. Introduction

The current Novel Corona Virus (2019-nCoV) infection has caused a global emergency by driving widespread across the globe in a short period. Infection-induced mortality is also very high. In December 2019, Wuhan, China, marks the start of a new coronavirus outbreak [1, 2]. The World Health Organization (WHO) proclaimed the infection a pandemic on March 11, 2020 [3]. The most prevalent symptoms include dry cough, fever, and breathing problems. Joint and muscle discomfort, sore throat, headache, and loss of smell or taste are among the symptoms. Social isolation, face masks, regular hand washing, reducing non-essential travel, case isolation, family quarantine, and the closure of schools and universities have all been used to prevent the spread of this fatal disease [4–7].

On January 30, 2020, the first symptom of COVID-19 was identified in India. The country disclosed its first three instances in Kerala; all three cases involved college students who had just returned from Wuhan, China [8]. In March, transmission increased as several reported cases throughout the nation were related to individuals who had travelled to COVID-19 affected countries. Corona Virus Disease (COVID-19) has started spreading in a large number of positive cases from the first week of March 2020. India is a country with a high population density; due to this, India has a very high human-to-human social interaction rate. Therefore, controlling the COVID-19 pandemic in its early phases was a very urgent and severe challenge.

Vaccination is an essential public health technique in contemporary medicine that has been utilized to reduce the effect of numerous infectious illnesses [9,10]. A vaccine is any biologically generated material

* Corresponding author.
E-mail addresses: skumawatmath@gmail.com (Shyamsunder), jangidkamlesh7@gmail.com (K. Jangid), aabidemi@futa.edu.ng (A. Abidemi), kmowolabi@futa.edu.ng (K.M. Owolabi), sunil_a_purohit@yahoo.com (S.D. Purohit).

https://doi.org/10.1016/j.dajour.2022.100156
Received 5 October 2022; Received in revised form 16 December 2022; Accepted 22 December 2022
Available online 24 December 2022
2772-6622/© 2022 The Author(s). Published by Elsevier Inc. This is an open access article under the CC BY license (http://creativecommons.org/licenses/by/4.0/).

that generates a protective immune response when delivered to a vulnerable host. Vaccines assist the body in preparing for illness by using the fact that immunity understands how to resist infectious organisms, which are often viruses, bacteria, or toxins [11]. There is rising worry that vaccination may not result in herd immunity due to the introduction of highly transmissible novel variations, decreasing vaccine efficacy, and uneven vaccine availability. Vaccines minimize the probability of severe illness and death; hence, vaccination/immunization coverage must be high for a country's healthcare system to be protected against an infection spike. Getting vaccinated is a decision of social duty made by a person. However, the vaccine's anxiety and adverse side effects must be addressed [12].

A major problem has arisen worldwide. To overcome this problem, scientists and doctors worldwide started searching for anti-viral medicine or vaccine for this infection. India also succeeded in discovering such an infection and found a vaccine for the infection. The first vaccine was administered in India on 16 January 2021 [13]. After the first stage of vaccination, the second dose is given, which is given 3–4 weeks after the first vaccine [14]. In India, 90% of the population has received the first dose, and 70% have been given both doses of the vaccine [15]. However, the COVID-19 vaccines could not offer a 100% protection against the infection due to the discoveries of new variants [16]. This is evident from many cases of post-vaccination infections that have been reported. Thus, this paper aims to present a mathematical analysis of the post-vaccination transmission dynamic of COVID-19, particularly in India.

Mathematical models based on ordinary differential equations of integer order have been widely employed to study the dynamics of biological systems [17,18]. Based on the principles of mathematical epidemiology, a number of mathematical models for social epidemics (such as crime and drug abuse) has also been presented [19–22]. Every model is based on classical derivatives, with different constraints depending on the differential equation order. In many works [7,10,23–26,26,27], integer order mathematical models have been developed and rigorously analysed to gain insights into the transmission dynamic and control of COVID-19. For instance, Mishra et al. [23] developed a mathematical model of COVID-19 dynamics with categories including susceptible, isolation, exposed, asymptotic, infected, and recovered individuals. In [25], Džiugys et al. studied a simplified mathematical model for COVID-19 which takes into consideration the quarantine conditions. The work presented a method to estimate the effectiveness of quarantine. Biswas et al. [28] developed a deterministic compartmental model (DCM) and calculated the model's parameters using pandemic data from India.

To overcome the limitations of the integer order mathematical models, many authors have resorted to fractional calculus to overcome these restrictions. Fractional calculus differential operators describe non-local dynamics and unusual behaviour in natural phenomena, nature-related truths, and facts related to nature [29,30]. Non-integer or fractional sequences, memory, and natural phenomena make them suitable. Because these structures rely on the memory-constrained strength of a fractional derivative operator, the study of epidemiological dynamical processes incorporating memory effects is acceptable. Therefore, many researchers have examined fractional operator-based epidemic models for various infectious illnesses because they exhibit a plausible biphasic decline in disease transmission [31–37]. For instance, Peter and co-workers in [37] used a newly formulated non-integer order mathematical model incorporating the effects of vaccination and treatment under Atangana–Baleanu–Caputo derivative operator to study the transmission dynamic of meningitis in the population. The authors remarked that fractional parameter acts as a control parameter to identify important techniques for the disease control. To investigate the spread of COVID-19, various researchers have used fractional order mathematical models to describe the dynamics of COVID-19 [38–42]. Nabizadeh et al. [43] highlights the relapse of multiple sclerosis after COVID-19 immunization. Shaikh et al. [44] studied the dynamics of transmission and control of COVID-19 in India. In earlier studies, mathematical modelling helped to investigate India's COVID-19 vaccine development activities [45], people's attitudes regarding vaccinations [46], the most comprehensive vaccination programmes [47], and allocation tactics [48].

In a similar development, the authors in [49] presented a time-fractional compartmental model for the assessment of COVID-19 transmission dynamics in China. The closed-form series solution of the model was obtained using the multistage optimal homotopy asymptotic method. In [50], Agarwal et al. used a fractional-order mathematical model to facilitate a better understanding of the transmission dynamic of COVID-19 pandemic. To establish the existence and uniqueness of the model, the authors employed fixed-point theorem, while the approximate solution of the model was derived using the predictor–corrector algorithm. Zeb et al. [34] proposed a compartmental mathematical model of COVID-19 dynamics with quarantine class and vaccination. The stochastic version of the model was formulated by appropriately introducing environmental noises into the model. Furthermore, the fractional-order form of the proposed model was derived for the long term expansion under the Caputo–Fabrizio fractional derivative operator. Newton Polynomial scheme was employed to obtain the numerical solution to the fractional-order compartmental model. The work of Aldawish and Ibrahim [51] was focused on the formulation and analysis of a system of coupled differential equations which describes the dynamics of the diffusion between the infectious and asymptomatically infected people under ABC-fractional derivative operator.

Pandey et al. [52] proposed a non-integer order mathematical model capturing the crowding effects of SARS-CoV-2 virus under Atangana–Baleanu fractional derivative operator. The authors further explored the existence and uniqueness of their theoretical results using a fixed-point method. In Ali et al. [53], a fractional-order mathematical model of COVID-19 dynamic featuring the effect of symptomatic and asymptomatic transmissions under Caputo fractional derivative was developed and rigorously analysed in both qualitative and quantitative senses. The study of Owoyemi et al. [16] made a generalization of an integer-order mathematical model describing the transmission dynamics of COVID-19 to a fractional-order version in the sense of Caputo fractional derivative. In a similar study, El-Sayed et al. [54] presented a fractional-order compartmental model, which describes the transmission dynamics of COVID-19, in Caputo sense. Padmapriya and Kaliyappan [55] formulated a mathematical model with a Caputo fractional derivative under fuzzy sense to predict the trend of COVID-19 outbreaks, specifically in USA, India and Italy.

In this research, a DCM governed by a seven-dimensional system of fractional-order ordinary differential equations in Caputo sense is developed to examine the transmission dynamics of COVID-19 after vaccination. The model parameters are estimated by fitting the model to the available data on the current epidemic in India. Using real data, the basic reproduction number of the model is estimated to quantify the burden of the disease in the population. The remaining parts of this paper are structured as follows: Section 2 is dedicated to the formulation of the classical and the fractional-order COVID-19 models proposed in this work. Some useful definitions to our study are also presented. In Section 3, we derive the iterative scheme for the proposed Caputo fractional COVID-19 model, and established the stability of the model. Section 4 discusses the computation of the basic reproduction number of the model and its sensitivity to the model parameters. In Section 5, the numerical approximation technique for the Caputo fractional derivative is presented. We conduct data fitting and numerical simulations in Section 6. The results arising from the processes are also presented. Section 7 is based on detail discussion. The study is concluded in Section 8.

2. Model formulation

In this section, we will use a classical DCM to investigate the transmission mechanisms of COVID-19 following vaccination. The model will later be transformed into a fractional order version under Caputo fractional derivative operator.

2.1. Integer-order COVID-19 model

Here, we propose an integer-order DCM of COVID-19 dynamics which divided the total population at time t, denoted by (N), into seven groups: the susceptible people (S), exposed people (E), symptomatic infected people without taking any vaccine (U), symptomatic infected people after the first dose vaccination (V), symptomatic infected people after the second dose (full) vaccination (W), recovered people (R), and dead people (D), so that at any time t, the total human population is given by $N(t) = S(t) + E(t) + U(t) + V(t) + W(t) + R(t) + D(t)$.

Thus, the non-linear integer order compartmental mathematical model describing the transmission dynamics of COVID-19 in the population is presented by

$$\begin{aligned}
\frac{dS(t)}{dt} &= \zeta - (\varphi + \sigma)S,\\
\frac{dE(t)}{dt} &= \sigma S - (\varphi + \lambda_u + \lambda_v + \lambda_w)E,\\
\frac{dU(t)}{dt} &= \lambda_u E - (\varphi + \Lambda_u + \theta_u)U,\\
\frac{dV(t)}{dt} &= \lambda_v E - (\varphi + \Lambda_v + \theta_v)V,\\
\frac{dW(t)}{dt} &= \lambda_w E - (\varphi + \Lambda_w + \theta_w)W,\\
\frac{dR(t)}{dt} &= \Lambda_u U + \Lambda_v V + \Lambda_w W - \varphi R,\\
\frac{dD(t)}{dt} &= \theta_u U + \theta_v V + \theta_w W - \varphi D,
\end{aligned} \tag{1}$$

where σ is the power of the infection (rate at which susceptible people contract the disease from unvaccinated symptomatic individuals, symptomatic individuals after receiving the first dose vaccine and symptomatic individuals after receiving the second dose vaccine) expressed as

$$\sigma = \frac{\ell(U + \xi V + \beta W)}{N},$$

and with the non-negative initial conditions defined as

$$S(0) = S_0,\ E(0) = E_0,\ U(0) = U_0,\ V(0) = V_0,\ W(0) = W_0,\ R(0) = R_0,$$
$$D(0) = D_0.$$

Fig. 1 displays the schematic diagram of model (1). All the parameters of model (1) are described as follows:

ℓ	Is the rate of transmission (or contact rate),
ζ	Is the birth rate,
ξ	Is the modification factor for infected class V,
β	Is the modification factor for infected class W,
φ	Is the natural death rate,
$\lambda_u,\ \lambda_v,\ \lambda_w$	Are the rates of conversion from the exposed class E to U, V, W classes, respectively,
$\Lambda_u,\ \Lambda_v,\ \Lambda_w$	Are the recovery rates from U, V, W classes, respectively,
$\theta_u,\ \theta_v,\ \theta_w$	Are the Covid-19 disease mortality rates for individuals in U, V, W classes, respectively.

2.2. Mathematical preliminaries

In this section, certain definitions of fractional derivative operators namely, Caputo fractional derivative (CFD). The integral transforms required in forthcoming sections are also touched upon in this phase.

Definition 2.1 ([50,56,57]). The usual CFD is defined as follows:

$${}^{C}\mathfrak{D}^{\mu}_{\dagger}\, u(\dagger) = \frac{1}{\Gamma(1-\mu)} \int_0^{\dagger} u'(\zeta)\,(\dagger - \zeta)^{-\mu}\, d\zeta \quad ;\ \dagger \geq 0,\ 0 < \mu \leq 1. \tag{2}$$

Definition 2.2 ([58]). The Laplace transform of piecewise continuous function $h(x)$ of exponential order $\beta > 0$ with respect to variable x is defined as follows:

$$L[h(x); s] = \bar{h}(s) = \int_0^{\infty} e^{-s\,x}\, h(x)\, dx \quad ;\Re(s) > \beta,\ x \geq 0. \tag{3}$$

The inverse Laplace transform of function $\bar{g}(s)$ with respect to $y \geq 0$ is given by

$$L^{-1}[\bar{h}(s); x] = h(x) = \frac{1}{2\pi i} \int_{\gamma - i\infty}^{\gamma + i\infty} e^{h\,x}\, \bar{h}(s) ds, \tag{4}$$

where γ is the fixed real number.

Definition 2.3 ([59]). The Laplace transform of the CFD of order μ gives the following expression:

$$L\left[{}^{C}\mathfrak{D}^{\mu}_{\dagger}\, u(\dagger)\right](\mathfrak{p}) = \mathfrak{p}^{\mu} L[u(\dagger)] - \mathfrak{p}^{\mu-1}\, u(0). \tag{5}$$

2.3. The Caputo fractional COVID-19 model

This section discusses the formulation of fractional-order DCM of COVID-19. Using Definition 2.1, we then modulate the system (1) by replacing the time derivative with the CFD to arrive at the following non-linear fractional mathematical model of COVID-19 dynamics:

$$\begin{aligned}
{}^{C}\mathfrak{D}^{\mu}_{t}\, S(t) &= \zeta - (\varphi + \sigma)S,\\
{}^{C}\mathfrak{D}^{\mu}_{t}\, E(t) &= \sigma S - (\varphi + \lambda_u + \lambda_v + \lambda_w)E,\\
{}^{C}\mathfrak{D}^{\mu}_{t}\, U(t) &= \lambda_u E - (\varphi + \Lambda_u + \theta_u)U,\\
{}^{C}\mathfrak{D}^{\mu}_{t}\, V(t) &= \lambda_v E - (\varphi + \Lambda_v + \theta_v)V,\\
{}^{C}\mathfrak{D}^{\mu}_{t}\, W(t) &= \lambda_w E - (\varphi + \Lambda_w + \theta_w)W,\\
{}^{C}\mathfrak{D}^{\mu}_{t}\, R(t) &= \Lambda_u U + \Lambda_v V + \Lambda_w W - \varphi R,\\
{}^{C}\mathfrak{D}^{\mu}_{t}\, D(t) &= \theta_u U + \theta_v V + \theta_w W - \varphi D,
\end{aligned} \tag{6}$$

together with preliminary conditions at time $t = 0$, where μ is the order of CFD operator such that $\mu \in (0, 1]$.

3. Iterative scheme and stability analysis of the Caputo fractional COVID-19 model

3.1. Iterative scheme

Here, we follow the ideas of the authors in [44] to derive the iterative scheme for the Caputo fractional model (6). Consider the Covid-19 model (6) along with preliminary conditions. Taking the Laplace transforms on both sides of each fractional differential equation of system (6), we have

$$\begin{aligned}
\mathfrak{p}^{\mu}\,\mathscr{L}[S(t)] - \mathfrak{p}^{\mu-1}\, S(0) &= \mathscr{L}\Big[\zeta - (\varphi + \sigma)S\Big],\\
\mathfrak{p}^{\mu}\,\mathscr{L}[E(t)] - \mathfrak{p}^{\mu-1}\, E(0) &= \mathscr{L}\Big[\sigma S - (\varphi + \lambda_u + \lambda_v + \lambda_w)E\Big],\\
\mathfrak{p}^{\mu}\,\mathscr{L}[U(t)] - \mathfrak{p}^{\mu-1}\, U(0) &= \mathscr{L}\Big[\lambda_u E - (\varphi + \Lambda_u + \theta_u)U\Big],\\
\mathfrak{p}^{\mu}\,\mathscr{L}[V(t)] - \mathfrak{p}^{\mu-1}\, V(0) &= \mathscr{L}\Big[\lambda_v E - (\varphi + \Lambda_v + \theta_v)V\Big],\\
\mathfrak{p}^{\mu}\,\mathscr{L}[W(t)] - \mathfrak{p}^{\mu-1}\, W(0) &= \mathscr{L}\Big[\lambda_w E - (\varphi + \Lambda_w + \theta_w)W\Big],\\
\mathfrak{p}^{\mu}\,\mathscr{L}[R(t)] - \mathfrak{p}^{\mu-1}\, R(0) &= \mathscr{L}\Big[\Lambda_u U + \Lambda_v V + \Lambda_w W - \varphi R\Big],\\
\mathfrak{p}^{\mu}\,\mathscr{L}[D(t)] - \mathfrak{p}^{\mu-1}\, D(0) &= \mathscr{L}\Big[\theta_u U + \theta_v V + \theta_w W - \varphi D\Big].
\end{aligned} \tag{7}$$

Rearranging, we obtain

$$\begin{aligned}
\mathscr{L}\Big[S(t)\Big] &= \frac{S(0)}{\mathfrak{p}} + \frac{1}{\mathfrak{p}^{\mu}}\,\mathscr{L}\Big[\zeta - (\varphi + \sigma)S\Big],\\
\mathscr{L}\Big[E(t)\Big] &= \frac{E(0)}{\mathfrak{p}} + \frac{1}{\mathfrak{p}^{\mu}}\,\mathscr{L}\Big[\sigma S - (\varphi + \lambda_u + \lambda_v + \lambda_w)E\Big],\\
\mathscr{L}\Big[U(t)\Big] &= \frac{U(0)}{\mathfrak{p}} + \frac{1}{\mathfrak{p}^{\mu}}\,\mathscr{L}\Big[\lambda_u E - (\varphi + \Lambda_u + \theta_u)U\Big],\\
\mathscr{L}\Big[V(t)\Big] &= \frac{V(0)}{\mathfrak{p}} + \frac{1}{\mathfrak{p}^{\mu}}\,\mathscr{L}\Big[\lambda_v E - (\varphi + \Lambda_v + \theta_v)V\Big],\\
\mathscr{L}\Big[W(t)\Big] &= \frac{W(0)}{\mathfrak{p}} + \frac{1}{\mathfrak{p}^{\mu}}\,\mathscr{L}\Big[\lambda_w E - (\varphi + \Lambda_w + \theta_w)W\Big],\\
\mathscr{L}\Big[R(t)\Big] &= \frac{R(0)}{\mathfrak{p}} + \frac{1}{\mathfrak{p}^{\mu}}\,\mathscr{L}\Big[\Lambda_u U + \Lambda_v V + \Lambda_w W - \varphi R\Big],\\
\mathscr{L}\Big[D(t)\Big] &= \frac{D(0)}{\mathfrak{p}} + \frac{1}{\mathfrak{p}^{\mu}}\,\mathscr{L}\Big[\theta_u U + \theta_v V + \theta_w W - \varphi D\Big].
\end{aligned} \tag{8}$$

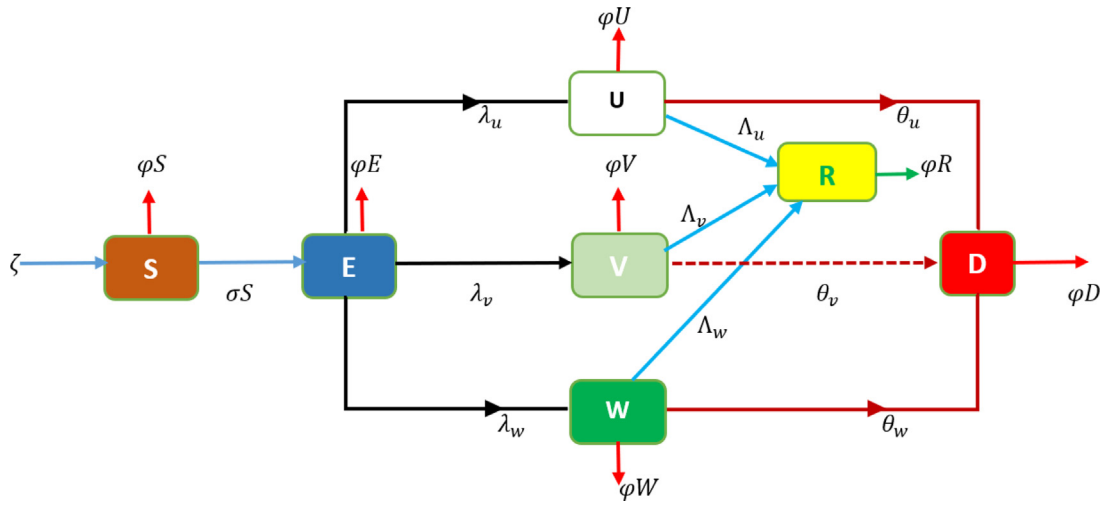

Fig. 1. Flow diagram of the SEUVWRD model.

Further analysis, by taking the inverse Laplace transforms of the equations in (8), yields

$$\begin{aligned}
S(t) &= S(0) + \mathscr{L}^{-1}\left[\frac{1}{\mathfrak{p}^{\mu}}\mathscr{L}\left[\zeta - (\varphi+\sigma)S\right]\right],\\
E(t) &= E(0) + \mathscr{L}^{-1}\left[\frac{1}{\mathfrak{p}^{\mu}}\mathscr{L}\left[\sigma S - (\varphi+\lambda_u+\lambda_v+\lambda_w)E\right]\right],\\
U(t) &= U(0) + \mathscr{L}^{-1}\left[\frac{1}{\mathfrak{p}^{\mu}}\mathscr{L}\left[\lambda_u E - (\varphi+\Lambda_u+\theta_u)U\right]\right],\\
V(t) &= V(0) + \mathscr{L}^{-1}\left[\frac{1}{\mathfrak{p}^{\mu}}\mathscr{L}\left[\lambda_v E - (\varphi+\Lambda_v+\theta_v)V\right]\right],\\
W(t) &= W(0) + \mathscr{L}^{-1}\left[\frac{1}{\mathfrak{p}^{\mu}}\mathscr{L}\left[\lambda_w E - (\varphi+\Lambda_w+\theta_w)W\right]\right],\\
R(t) &= R(0) + \mathscr{L}^{-1}\left[\frac{1}{\mathfrak{p}^{\mu}}\mathscr{L}\left[\Lambda_u U + \Lambda_v V + \Lambda_w W - \varphi R\right]\right],\\
D(t) &= D(0) + \mathscr{L}^{-1}\left[\frac{1}{\mathfrak{p}^{\mu}}\mathscr{L}\left[\theta_u U + \theta_v V + \theta_w W - \varphi D\right]\right].
\end{aligned} \tag{9}$$

Consequently, the series solutions obtained by the procedure are denoted by

$$\begin{aligned}
&S = \sum_{n=0}^{\infty} S_n,\ E = \sum_{n=0}^{\infty} E_n,\ U = \sum_{n=0}^{\infty} U_n,\ V = \sum_{n=0}^{\infty} V_n,\ W = \sum_{n=0}^{\infty} W_n,\\
&R = \sum_{n=0}^{\infty} R_n,\ D = \sum_{n=0}^{\infty} D_n.
\end{aligned} \tag{10}$$

Using the preliminary conditions, we obtain the recursive formula given as

$$\begin{aligned}
S_{n+1}(t) &= S_n(0) + \mathscr{L}^{-1}\left[\frac{1}{\mathfrak{p}^{\mu}}\mathscr{L}\left[\zeta - (\varphi+\sigma)S_n\right]\right],\\
E_{n+1}(t) &= E_n(0) + \mathscr{L}^{-1}\left[\frac{1}{\mathfrak{p}^{\mu}}\mathscr{L}\left[\sigma S_n - (\varphi+\lambda_u+\lambda_v+\lambda_w)E_n\right]\right],\\
U_{n+1}(t) &= U_n(0) + \mathscr{L}^{-1}\left[\frac{1}{\mathfrak{p}^{\mu}}\mathscr{L}\left[\lambda_u E_n - (\varphi+\Lambda_u+\theta_u)U_n\right]\right],\\
V_{n+1}(t) &= V_n(0) + \mathscr{L}^{-1}\left[\frac{1}{\mathfrak{p}^{\mu}}\mathscr{L}\left[\lambda_v E_n - (\varphi+\Lambda_v+\theta_v)V_n\right]\right],\\
W_{n+1}(t) &= W_n(0) + \mathscr{L}^{-1}\left[\frac{1}{\mathfrak{p}^{\mu}}\mathscr{L}\left[\lambda_w E_n - (\varphi+\Lambda_w+\theta_w)W_n\right]\right],\\
R_{n+1}(t) &= R_n(0) + \mathscr{L}^{-1}\left[\frac{1}{\mathfrak{p}^{\mu}}\mathscr{L}\left[\Lambda_u U_n + \Lambda_v V_n + \Lambda_w W_n - \varphi R_n\right]\right],\\
D_{n+1}(t) &= D_n(0) + \mathscr{L}^{-1}\left[\frac{1}{\mathfrak{p}^{\mu}}\mathscr{L}\left[\theta_u U_n + \theta_v V_n + \theta_w W_n - \varphi D_n\right]\right].
\end{aligned} \tag{11}$$

3.2. Stability analysis

In this part, details of the stability analysis of the Caputo fractional COVID-19 model (2) is presented by following the idea reported in previous works [50,53,57,60]. Now, consider $(\daleth, \|.\|)$ to be a Banach space with a self-map $\acute{T}$ on $\daleth$. In addition, consider $\mathscr{X}_{n+1} = p(\acute{T}, \mathscr{X}_n)$ to be an exact recurrence formula. $\mathcal{U}(\acute{T})$ represents a fixed point set of $\acute{T}$. Furthermore, $\acute{T}$ contains at least one element ζ_n, that converges to the point $y \in \mathcal{U}(\acute{T})$. Let $\{x_n \in \daleth\}$ and define $z_n = \|x_{n+1} - p(\acute{T}, x_n)\|$. When $\lim_{n\to\infty} z^n = 0$, $\lim_{n\to\infty} x^n = y$, an iteration method $\mathscr{X}_{n+1} = p(\acute{T}, \mathscr{X}_n)$ is known as $\acute{T}-$stable. The sequence $\{x_n\}$ has an upper bound, and the iteration is referred to as Picard's iteration. Additionally, it is $\acute{T}-$ stable. It satisfies the above specifications for $\mathscr{X}_{n+1} = \acute{T}\mathscr{X}_n$.

Proposition 3.1. *Assuming $(\daleth, \|.\|)$ is a Banach space, F is a self-map on $\daleth$ and satisfies $\|F_a - F_b\| \le \xi\|a - F_a\| + \rho\|a - b\| \quad \forall a, b \in \daleth$ with $0 \le \xi$, $0 \le \rho < 1$. Then, we say that F is Picard F-stable.*

Furthermore, consider the relationship between (11) and (6). The following proposition holds:

Proposition 3.2. *Consider the following self-map F*

$$\begin{aligned}
F(S_n(t)) &= S_{n+1}(t),\\
&= S_n(0) + \mathscr{L}^{-1}\left[\frac{1}{\mathfrak{p}^{\mu}}\mathscr{L}\left[\zeta - (\varphi+\sigma)S_n\right]\right],\\
F(E_n(t)) &= E_{n+1}(t),\\
&= E_n(0) + \mathscr{L}^{-1}\left[\frac{1}{\mathfrak{p}^{\mu}}\mathscr{L}\left[\sigma S_n - (\varphi+\lambda_u+\lambda_v+\lambda_w)E_n\right]\right],\\
F(U_n(t)) &= U_{n+1}(t),\\
&= U_n(0) + \mathscr{L}^{-1}\left[\frac{1}{\mathfrak{p}^{\mu}}\mathscr{L}\left[\lambda_u E_n - (\varphi+\Lambda_u+\theta_u)U_n\right]\right],\\
F(V_n(t)) &= V_{n+1}(t),\\
&= V_n(0) + \mathscr{L}^{-1}\left[\frac{1}{\mathfrak{p}^{\mu}}\mathscr{L}\left[\lambda_v E_n - (\varphi+\Lambda_v+\theta_v)V_n\right]\right],\\
F(W_n(t)) &= W_{n+1}(t),\\
&= W_n(0) + \mathscr{L}^{-1}\left[\frac{1}{\mathfrak{p}^{\mu}}\mathscr{L}\left[\lambda_w E_n - (\varphi+\Lambda_w+\theta_w)W_n\right]\right],\\
F(R_n(t)) &= R_{n+1}(t),\\
&= R_n(0) + \mathscr{L}^{-1}\left[\frac{1}{\mathfrak{p}^{\mu}}\mathscr{L}\left[\Lambda_u U_n + \Lambda_v V_n + \Lambda_w W_n - \varphi R_n\right]\right],\\
F(D_n(t)) &= D_{n+1}(t),\\
&= D_n(0) + \mathscr{L}^{-1}\left[\frac{1}{\mathfrak{p}^{\mu}}\mathscr{L}\left[\theta_u U_n + \theta_v V_n + \theta_w W_n - \varphi D_n\right]\right],
\end{aligned}$$

in $L^1(a,b)$. *Then, it is* F*-stable if*

$$\begin{aligned}
&\Big(1-(\varphi+\sigma)G(\mu)\Big)<1,\\
&\Big(1+\sigma G_1(\mu)-\big(\varphi+\lambda_u+\lambda_v+\lambda_w\big)H(\mu)\Big)<1,\\
&\Big(1+\lambda_u H_1(\mu)-\big(\varphi+\Lambda_u+\theta_u\big)I(\mu)\Big)<1,\\
&\Big(1+\lambda_v H_2(\mu)-(\varphi+\Lambda_v+\theta_v)J(\mu)\Big)<1,\\
&\Big(1+\lambda_w H_3(\mu)-\big(\varphi+\Lambda_w+\theta_w\big)K(\mu)\Big)<1,\\
&\Big(1+\Lambda_u I_1(\mu)+\Lambda_v J_1(\mu)+\Lambda_w K_1(\mu)-\varphi L(\mu)\Big)<1,\\
&\Big(1+\theta_u I_2(\mu)+\theta_v J_2(\mu)+\theta_w K_2(\mu)-\varphi M(\mu)\Big)<1.
\end{aligned}\tag{12}$$

Proof. The proof begins by showing that F has a fixed point. Therefore, for all $(m,n)\in N\times N$, we evaluate the following differences:

$$\begin{aligned}
F\big(S_m(t)\big)-F\big(S_n(t)\big)&=S_m(0)-S_n(0)+\mathscr{L}^{-1}\Big[\frac{1}{\mathrm{p}^\mu}\mathscr{L}\big[\zeta-(\varphi+\sigma)S_m\big]\Big]\\
&\quad-\mathscr{L}^{-1}\Big[\frac{1}{\mathrm{p}^\mu}\mathscr{L}\big[\zeta-(\varphi+\sigma)S_n\big]\Big],\\
F\big(E_m(t)\big)-F\big(E_n(t)\big)&=E_m(0)-E_n(0)\\
&\quad+\mathscr{L}^{-1}\Big[\frac{1}{\mathrm{p}^\mu}\mathscr{L}\big[\sigma S_m-(\varphi+\lambda_u+\lambda_v+\lambda_w)E_m\big]\Big]\\
&\quad-\mathscr{L}^{-1}\Big[\frac{1}{\mathrm{p}^\mu}\mathscr{L}\big[\sigma S_n-(\varphi+\lambda_u+\lambda_v+\lambda_w)E_n\big]\Big],\\
F\big(U_m(t)\big)-F\big(U_n(t)\big)&=U_m(0)-U_n(0)\\
&\quad+\mathscr{L}^{-1}\Big[\frac{1}{\mathrm{p}^\mu}\mathscr{L}\big[\lambda_u E_m-(\varphi+\Lambda_u+\theta_u)U_m\big]\Big]\\
&\quad-\mathscr{L}^{-1}\Big[\frac{1}{\mathrm{p}^\mu}\mathscr{L}\big[\lambda_u E_n-(\varphi+\Lambda_u+\theta_u)U_n\big]\Big],\\
F\big(V_m(t)\big)-F\big(V_n(t)\big)&=V_m(0)-V_n(0)\\
&\quad+\mathscr{L}^{-1}\Big[\frac{1}{\mathrm{p}^\mu}\mathscr{L}\big[\lambda_v E_m-(\varphi+\Lambda_v+\theta_v)V_m\big]\Big]\\
&\quad-\mathscr{L}^{-1}\Big[\frac{1}{\mathrm{p}^\mu}\mathscr{L}\big[\lambda_v E_n-(\varphi+\Lambda_v+\theta_v)V_n\big]\Big],\\
F\big(W_m(t)\big)-F\big(W_n(t)\big)&=W_m(0)-W_n(0)\\
&\quad+\mathscr{L}^{-1}\Big[\frac{1}{\mathrm{p}^\mu}\mathscr{L}\big[\lambda_w E_m-(\varphi+\Lambda_w+\theta_w)W_m\big]\Big]\\
&\quad-\mathscr{L}^{-1}\Big[\frac{1}{\mathrm{p}^\mu}\mathscr{L}\big[\lambda_w E_n-(\varphi+\Lambda_w+\theta_w)W_n\big]\Big],\\
F\big(R_m(t)\big)-F\big(R_n(t)\big)&=R_m(0)-R_n(0)\\
&\quad+\mathscr{L}^{-1}\Big[\frac{1}{\mathrm{p}^\mu}\mathscr{L}\big[\Lambda_u U_m+\Lambda_v V_m+\Lambda_w W_m-\varphi R_m\big]\Big]\\
&\quad-\mathscr{L}^{-1}\Big[\frac{1}{\mathrm{p}^\mu}\mathscr{L}\big[\Lambda_u U_n+\Lambda_v V_n+\Lambda_w W_n-\varphi R_n\big]\Big],\\
F\big(D_m(t)\big)-F\big(D_n(t)\big)&=D_m(0)-D_n(0)\\
&\quad+\mathscr{L}^{-1}\Big[\frac{1}{\mathrm{p}^\mu}\mathscr{L}\big[\theta_u U_m+\theta_v V_m+\theta_w W_m-\varphi D_m\big]\Big]\\
&\quad-\mathscr{L}^{-1}\Big[\frac{1}{\mathrm{p}^\mu}\mathscr{L}\big[\theta_u U_n+\theta_v V_n+\theta_w W_n-\varphi D_n\big]\Big].
\end{aligned}\tag{13}$$

Taking the norm of each side of the first equation of (13) without losing generality, we obtain

$$\begin{aligned}
\|F\big(S_m(t)\big)-F\big(S_n(t)\big)\|&=\Big\|S_m(0)-S_n(0)+\mathscr{L}^{-1}\Big[\frac{1}{\mathrm{p}^\mu}\mathscr{L}\big[\zeta-(\varphi+\sigma)S_m\big]\Big]\\
&\quad-\mathscr{L}^{-1}\Big[\frac{1}{\mathrm{p}^\mu}\mathscr{L}\big[\zeta-(\varphi+\sigma)S_n\big]\Big]\Big\|.
\end{aligned}\tag{14}$$

Consequently, utilizing triangular inequality and further simplifying Eq. (14) yield the following result:

$$\begin{aligned}
\|F\big(S_m(t)\big)-F\big(S_n(t)\big)\|&\le\|S_m(0)-S_n(0)\|\\
&\quad+\mathscr{L}^{-1}\Big[\frac{1}{\mathrm{p}^\mu}\mathscr{L}\big[\|-(\varphi+\sigma)(S_m-S_n)\|\big]\Big],
\end{aligned}$$

or

$$\|F\big(S_m(t)\big)-F\big(S_n(t)\big)\|\le\big(1-(\varphi+\sigma)G(\mu)\big)\|S_m-S_n\|.\tag{15}$$

Similarly, we can obtain

$$\begin{aligned}
\|F\big(E_m(t)\big)-F\big(E_n(t)\big)\|&\le\Big(1+\sigma G_1(\mu)-\big(\varphi+\lambda_u+\lambda_v+\lambda_w\big)H(\mu)\Big)\\
&\quad\times\|E_m-E_n\|,\\
\|F\big(U_m(t)\big)-F\big(U_n(t)\big)\|&\le\Big(1+\lambda_u H_1(\mu)-\big(\varphi+\Lambda_u+\theta_u\big)I(\mu)\Big)\\
&\quad\times\|U_m-U_n\|,\\
\|F\big(V_m(t)\big)-F\big(V_n(t)\big)\|&\le\Big(1+\lambda_v H_2(\mu)-(\varphi+\Lambda_v+\theta_v)J(\mu)\Big)\\
&\quad\times\|V_m-V_n\|,\\
\|F\big(W_m(t)\big)-F\big(W_n(t)\big)\|&\le\Big(1+\lambda_w H_3(\mu)-\big(\varphi+\Lambda_w+\theta_w\big)K(\mu)\Big)\\
&\quad\times\|W_m-W_n\|,\\
\|F\big(R_m(t)\big)-F\big(R_n(t)\big)\|&\le\Big(1+\Lambda_u I_1(\mu)+\Lambda_v J_1(\mu)+\Lambda_w K_1(\mu)-\varphi L(\mu)\Big)\\
&\quad\times\|R_m-R_n\|,\\
\|F\big(D_m(t)\big)-F\big(D_n(t)\big)\|&\le\Big(1+\theta_u I_2(\mu)+\theta_v J_2(\mu)+\theta_w K_2(\mu)-\varphi M(\mu)\Big)\\
&\quad\times\|D_m-D_n\|,
\end{aligned}\tag{16}$$

where

$$\begin{aligned}
&\Big(1-(\varphi+\sigma)G(\mu)\Big)<1,\\
&\Big(1+\sigma G_1(\mu)-\big(\varphi+\lambda_u+\lambda_v+\lambda_w\big)H(\mu)\Big)<1,\\
&\Big(1+\lambda_u H_1(\mu)-\big(\varphi+\Lambda_u+\theta_u\big)I(\mu)\Big)<1,\\
&\Big(1+\lambda_v H_2(\mu)-(\varphi+\Lambda_v+\theta_v)J(\mu)\Big)<1,\\
&\Big(1+\lambda_w H_3(\mu)-\big(\varphi+\Lambda_w+\theta_w\big)K(\mu)\Big)<1,\\
&\Big(1+\Lambda_u I_1(\mu)+\Lambda_v J_1(\mu)+\Lambda_w K_1(\mu)-\varphi L(\mu)\Big)<1,\\
&\Big(1+\theta_u I_2(\mu)+\theta_v J_2(\mu)+\theta_w K_2(\mu)-\varphi M(\mu)\Big)<1.
\end{aligned}$$

Therefore, the self mapping F has a fixed point. We show that F fulfils all of the prerequisites in Proposition 3.1. Assuming (15) and (16) hold, we use $\rho=(0,0,0,0,0,0,0)$ and

$$\xi=\begin{cases}
\Big(1-(\varphi+\sigma)G(\mu)\Big)<1,\\
\Big(1+\sigma G_1(\mu)-\big(\varphi+\lambda_u+\lambda_v+\lambda_w\big)H(\mu)\Big)<1,\\
\Big(1+\lambda_u H_1(\mu)-\big(\varphi+\Lambda_u+\theta_u\big)I(\mu)\Big)<1,\\
\Big(1+\lambda_v H_2(\mu)-(\varphi+\Lambda_v+\theta_v)J(\mu)\Big)<1,\\
\Big(1+\lambda_w H_3(\mu)-\big(\varphi+\Lambda_w+\theta_w\big)K(\mu)\Big)<1,\\
\Big(1+\Lambda_u I_1(\mu)+\Lambda_v J_1(\mu)+\Lambda_w K_1(\mu)-\varphi L(\mu)\Big)<1,\\
\Big(1+\theta_u I_2(\mu)+\theta_v J_2(\mu)+\theta_w K_2(\mu)-\varphi M(\mu)\Big)<1.
\end{cases}$$

Thus, each condition in Proposition 3.2 is satisfied by the self-map F. Hence, F is Picard F-stable. □

4. Basic reproduction number and sensitivity analysis

4.1. Basic reproduction number

To derive the basic reproduction number associated with model (6), it is necessary to first find the disease-free equilibrium of the model. By disease-free equilibrium, we mean the case when there are no infections in the population. Thus, all the contagious compartments of model (6) are set to zero. That is, $E=U=V=W=0$. Also, setting to zero the fractional derivatives of non-infectious compartments in model (6)'s

equations. That is, ${}^{C}\mathfrak{D}_t^{\mu} S(t) = {}^{C}\mathfrak{D}_t^{\mu} D(t) = 0$. Hence, the disease-free equilibrium point, denoted as $\mathfrak{Z}_0$, is given by

$$\mathfrak{Z}_0 = \left(S^0,\ E^0,\ U^0,\ V^0,\ W^0,\ R^0,\ D^0\right) = \left(\frac{\zeta}{\varphi},\ 0,\ 0,\ 0,\ 0,\ 0,\ 0\right). \quad (17)$$

Now, we use the next generation matrix approach as described in [61] to derive the basic reproduction number for model (6). In view of this approach, the matrix $\mathcal{A}$ of the new infection terms evaluated at $\mathfrak{Z}_0$ is given by

$$\mathcal{A} = \begin{pmatrix} 0 & \ell & \xi\ell & \beta\ell & 0 \\ 0 & 0 & 0 & 0 & 0 \\ 0 & 0 & 0 & 0 & 0 \\ 0 & 0 & 0 & 0 & 0 \\ 0 & 0 & 0 & 0 & 0 \end{pmatrix},$$

and the matrix $\mathcal{K}$ of the transition terms at the given point $\mathfrak{Z}_0$ is obtained as

$$\mathcal{K} = \begin{pmatrix} b_1 & 0 & 0 & 0 & 0 \\ -\lambda_u & b_2 & 0 & 0 & 0 \\ -\lambda_v & 0 & b_3 & 0 & 0 \\ -\lambda_w & 0 & 0 & b_4 & 0 \\ 0 & -\Lambda_u & -\Lambda_v & -\Lambda_w & \varphi \end{pmatrix},$$

where $b_1 = (\varphi + \lambda_u + \lambda_v + \lambda_w)$, $b_2 = (\varphi + \Lambda_u + \theta_u)$, $b_3 = (\varphi + \Lambda_v + \theta_v)$, $b_4 = (\varphi + \Lambda_w + \theta_w)$. Then, the largest eigenvalue of the next generation matrix $\mathcal{A}\mathcal{K}^{-1}$ is the needed effective reproduction number which is given by

$$\mathcal{R}_0 = \frac{\ell\lambda_u}{b_1 b_2} + \frac{\ell\xi\lambda_v}{b_1 b_3} + \frac{\ell\beta\lambda_w}{b_1 b_4}. \quad (18)$$

Three effective reproduction numbers are comprised in Eq. (18). The first number is $\mathcal{R}_{0U} = \frac{\ell\lambda_u}{b_1 b_2}$, it is defined as the number of new COVID-19 cases generated from the without taking any vaccine class of infected individuals (U), the second number is $\mathcal{R}_{0V} = \frac{\ell\xi\lambda_v}{b_1 b_3}$ defined as the number of cases generated from the first dose vaccination class of infected individuals (V) and the third number is $\mathcal{R}_{0W} = \frac{\ell\beta\lambda_w}{b_1 b_4}$, and it defines the number of COVID-19 cases generated from the second dose (full) immunization class of infected individuals (W). Thus, the expression for $\mathcal{R}_0$ in Eq. (18) can be written as

$$\mathcal{R}_0 = \mathcal{R}_{0U} + \mathcal{R}_{0V} + \mathcal{R}_{0W}. \quad (19)$$

4.2. Sensitivity analysis

In this section, the effects of all parameters associated with the basic reproduction number $\mathcal{R}_0$ as expressed in (18) are evaluated with a view to exploring the possible intervention strategies needed to prevent and control COVID-19 transmission in a population. For this purpose, we follow the ideas of authors in [19,50,53,54] in order to obtain the sensitivity of $\mathcal{R}_0$ in terms of each of its parameters with the use of the analytical expression given as

$$S_p^{\mathcal{R}_0} = \frac{p}{\mathcal{R}_0} \times \frac{\partial \mathcal{R}_0}{\partial p}, \quad (20)$$

where p is any parameter contained in $\mathcal{R}_0$. According to the relation (20), we obtain the analytical sensitivity indices of the reproduction number $\mathcal{R}_0$ with respect to the parameters of model (6) as follows:

$$S_{\ell}^{\mathcal{R}_0} = \frac{\ell}{\mathcal{R}_0}\left[\frac{\lambda_u}{b_1 b_2} + \frac{\xi\lambda_v}{b_1 b_3} + \frac{\beta\lambda_w}{b_1 b_4}\right],$$

$$S_{\xi}^{\mathcal{R}_0} = \frac{\xi}{\mathcal{R}_0}\left[\frac{\ell\lambda_v}{b_1 b_3}\right],$$

$$S_{\beta}^{\mathcal{R}_0} = \frac{\beta}{\mathcal{R}_0}\left[\frac{\ell\lambda_w}{b_1 b_4}\right],$$

$$S_{\varphi}^{\mathcal{R}_0} = \frac{\varphi}{\mathcal{R}_0}\left[-\frac{\ell\lambda_u}{b_1^2 b_2} - \frac{\ell\lambda_u}{b_1 b_2^2} - \frac{\ell\xi\lambda_v}{b_1^2 b_3} - \frac{\ell\xi\lambda_v}{b_1 b_2^2} - \frac{\ell\beta\lambda_w}{b_1^2 b_4} - \frac{\ell\beta\lambda_w}{b_1 b_4^2}\right],$$

$$S_{\lambda_u}^{\mathcal{R}_0} = \frac{\lambda_u}{\mathcal{R}_0}\left[\frac{\ell}{b_1 b_2} - \frac{\ell\lambda_u}{b_1^2 b_2} - \frac{\ell\xi\lambda_v}{b_1^2 b_3} - \frac{\ell\beta\lambda_w}{b_1^2 b_4}\right],$$

$$S_{\lambda_v}^{\mathcal{R}_0} = \frac{\lambda_v}{\mathcal{R}_0}\left[-\frac{\ell\lambda_u}{b_1^2 b_2} + \frac{\ell\xi}{b_1 b_3} - \frac{\ell\xi\lambda_v}{b_1^2 b_3} - \frac{\ell\beta\lambda_w}{b_1^2 b_4}\right],$$

$$S_{\lambda_w}^{\mathcal{R}_0} = \frac{\lambda_w}{\mathcal{R}_0}\left[-\frac{\ell\lambda_u}{b_1^2 b_2} - \frac{\ell\xi\lambda_v}{b_1^2 b_3} + \frac{\ell\beta}{b_1 b_4} - \frac{\ell\beta\lambda_w}{b_1^2 b_4}\right],$$

$$S_{\Lambda_u}^{\mathcal{R}_0} = \frac{\Lambda_u}{\mathcal{R}_0}\left[-\frac{\ell\lambda_u}{b_1 b_2^2}\right],$$

$$S_{\Lambda_v}^{\mathcal{R}_0} = \frac{\Lambda_v}{\mathcal{R}_0}\left[-\frac{\ell\xi\lambda_v}{b_1 b_3^2}\right],$$

$$S_{\Lambda_w}^{\mathcal{R}_0} = \frac{\Lambda_w}{\mathcal{R}_0}\left[-\frac{\ell\beta\lambda_w}{b_1 b_4^2}\right],$$

$$S_{\theta_u}^{\mathcal{R}_0} = \frac{\theta_u}{\mathcal{R}_0}\left[-\frac{\ell\lambda_u}{b_1 b_2^2}\right],$$

$$S_{\theta_v}^{\mathcal{R}_0} = \frac{\theta_v}{\mathcal{R}_0}\left[-\frac{\ell\xi\lambda_v}{b_1 b_3^2}\right],$$

$$S_{\theta_w}^{\mathcal{R}_0} = \frac{\theta_w}{\mathcal{R}_0}\left[-\frac{\ell\beta\lambda_w}{b_1 b_4^2}\right].$$

Therefore, the numerical sensitivity indexes of model (6), using $\mathcal{R}_0$ as a response function, are obtained by evaluating the above analytical results at the baseline values of the model parameters presented in Table 1. The results obtained are shown in Fig. 3.

5. Numerical scheme

Here, we present the numerical scheme for our suggested fractional model for the dynamics of COVID-19 dissemination after vaccination. By following the idea reported in [50,54,62], we consider the Cauchy problem associated with the CFD given as

$${}_0^{c}\mathfrak{D}_t^{\mu}\,\mathfrak{V}(t) = \mathscr{X}(t, \mathfrak{V}(t)),\ \ \mathfrak{V}(0) = \mathfrak{V}_0. \quad (21)$$

The Cauchy problem (21) is transformed by using the Caputo integral

$$\mathfrak{V}(t) - \mathfrak{V}(0) = \frac{1}{\Gamma(\mu)}\int_0^t \mathscr{X}(\zeta, \mathfrak{V}(\zeta))\,(t-\zeta)^{\mu-1}\,d\zeta. \quad (22)$$

At the point $t_{j+1} = (j+1)h$ and $t_j = jh$, $j = 0, 1, 2, \ldots$ with h being the time step, Eq. (22) is formulated as

$$\mathfrak{V}(t_{j+1}) - \mathfrak{V}(0) = \frac{1}{\Gamma(\mu)}\int_0^{t_{j+1}} \mathscr{X}(\zeta, \mathfrak{V}(\zeta))\,(t_{j+1}-\zeta)^{\mu-1}\,d\zeta, \quad (23)$$

which can be written as

$$\mathfrak{V}(t_{j+1}) = \mathfrak{V}(0) + \frac{1}{\Gamma(\mu)}\int_0^{t_{j+1}} \mathscr{X}(\zeta, \mathfrak{V}(\zeta))\,(t_{j+1}-\zeta)^{\mu-1}\,d\zeta. \quad (24)$$

Using the Lagrange polynomial [19,20,33,54], and simplifying the integral on the right side, Eq. (24) is changed into Eq. (25).

$$\mathfrak{V}_{j+1} = \mathfrak{V}_0 + \frac{1}{\Gamma(\mu)}\sum_{r=0}^{j}\left[\frac{\mathscr{X}(t_r, \mathfrak{V}_r)}{h}\int_{t_j}^{t_{j+1}} (\zeta - t_{r-1})\,(t_{j+1}-\zeta)^{\mu-1}\,d\zeta - \frac{\mathscr{X}(t_{r-1}, \mathfrak{V}_{r-1})}{h}\int_{t_j}^{t_{j+1}} (\zeta - t_r)\,(t_{j+1}-\zeta)^{\mu-1}\,d\zeta\right]. \quad (25)$$

Simplification of Eq. (25) yields the following numerical approach for the Caputo derivative:

$$\mathfrak{V}_{j+1} = \mathfrak{V}_0 + \frac{h^{\mu}}{\Gamma(\mu+2)}\sum_{r=0}^{j}\mathscr{X}(t_r, \mathfrak{V}_r)\left[(j-r+1)^{\mu}(j-r+2+\mu) - (j-r)^{\mu}(j-r+2+2\mu)\right] - \frac{h^{\mu}}{\Gamma(\mu+2)}\sum_{r=0}^{j}\mathscr{X}(t_{r-1}, \mathfrak{V}_{r-1})\left[(j-r+1)^{\mu+1} - (j-r)^{\mu}(j-r+1+\mu)\right]. \quad (26)$$

Thus, in terms of our model, we get

$$S_{j+1} = S_0 + \frac{h^\mu}{\Gamma(\mu+2)} \sum_{r=0}^{j} \mathscr{X}(t_r, S_r) \left[(j-r+1)^\mu (j-r+2+\mu) - (j-r)^\mu (j-r+2+2\mu) \right] - \frac{h^\mu}{\Gamma(\mu+2)} \sum_{r=0}^{j} \mathscr{X}(t_{r-1}, S_{r-1}) \left[(j-r+1)^{\mu+1} - (j-r)^\mu (j-r+1+\mu) \right],$$

$$E_{j+1} = E_0 + \frac{h^\mu}{\Gamma(\mu+2)} \sum_{r=0}^{j} \mathscr{X}(t_r, E_r) \left[(j-r+1)^\mu (j-r+2+\mu) - (j-r)^\mu (j-r+2+2\mu) \right] - \frac{h^\mu}{\Gamma(\mu+2)} \sum_{r=0}^{j} \mathscr{X}(t_{r-1}, E_{r-1}) \left[(j-r+1)^{\mu+1} - (j-r)^\mu (j-r+1+\mu) \right],$$

$$U_{j+1} = U_0 + \frac{h^\mu}{\Gamma(\mu+2)} \sum_{r=0}^{j} \mathscr{X}(t_r, U_r) \left[(j-r+1)^\mu (j-r+2+\mu) - (j-r)^\mu (j-r+2+2\mu) \right] - \frac{h^\mu}{\Gamma(\mu+2)} \sum_{r=0}^{j} \mathscr{X}(t_{r-1}, U_{r-1}) \left[(j-r+1)^{\mu+1} - (j-r)^\mu (j-r+1+\mu) \right],$$

$$V_{j+1} = V_0 + \frac{h^\mu}{\Gamma(\mu+2)} \sum_{r=0}^{j} \mathscr{X}(t_r, V_r) \left[(j-r+1)^\mu (j-r+2+\mu) - (j-r)^\mu (j-r+2+2\mu) \right] - \frac{h^\mu}{\Gamma(\mu+2)} \sum_{r=0}^{j} \mathscr{X}(t_{r-1}, V_{r-1}) \left[(j-r+1)^{\mu+1} - (j-r)^\mu (j-r+1+\mu) \right],$$

$$W_{j+1} = W_0 + \frac{h^\mu}{\Gamma(\mu+2)} \sum_{r=0}^{j} \mathscr{X}(t_r, W_r) \left[(j-r+1)^\mu (j-r+2+\mu) - (j-r)^\mu (j-r+2+2\mu) \right] - \frac{h^\mu}{\Gamma(\mu+2)} \sum_{r=0}^{j} \mathscr{X}(t_{r-1}, W_{r-1}) \left[(j-r+1)^{\mu+1} - (j-r)^\mu (j-r+1+\mu) \right],$$

$$R_{j+1} = R_0 + \frac{h^\mu}{\Gamma(\mu+2)} \sum_{r=0}^{j} \mathscr{X}(t_r, R_r) \left[(j-r+1)^\mu (j-r+2+\mu) - (j-r)^\mu (j-r+2+2\mu) \right] - \frac{h^\mu}{\Gamma(\mu+2)} \sum_{r=0}^{j} \mathscr{X}(t_{r-1}, R_{r-1}) \left[(j-r+1)^{\mu+1} - (j-r)^\mu (j-r+1+\mu) \right],$$

$$D_{j+1} = D_0 + \frac{h^\mu}{\Gamma(\mu+2)} \sum_{r=0}^{j} \mathscr{X}(t_r, D_r) \left[(j-r+1)^\mu (j-r+2+\mu) - (j-r)^\mu (j-r+2+2\mu) \right] - \frac{h^\mu}{\Gamma(\mu+2)} \sum_{r=0}^{j} \mathscr{X}(t_{r-1}, D_{r-1}) \left[(j-r+1)^{\mu+1} - (j-r)^\mu (j-r+1+\mu) \right].$$

It is worthy to mention that different numerical techniques apart from Lagrange polynomial, such as modified Euler's method, Adams–Bashforth scheme and Newton polynomial among others, have been considered to approximate problem of the form (21) by many authors [50,60,63].

6. Data fitting, numerical simulations and results

Using data for the estimation of some unknown parameters used in the construction of the model is an important step to take during model validation. In particular, the proposed model is calibrated to gain insights into the COVID-19 burden in terms of the newly daily infected cases during the vaccination regime. In this context, we make use of the publicly available daily reported COVID-19 cases data for India between 01 August 2021 and 21 July 2022, as published in [15].

Table 1
Estimated parameter values of model (Fig. 1).

Parameter	Value	Source
φ	$1/(69.66\times365)$	[15]
ζ	54 802.74	Estimated from [15]
λ_u	0.0236	Fitted
λ_v	0.0131	Fitted
λ_w	0.0121	Fitted
θ_u	0.0105	Estimated from [15]
θ_v	0.0036	Fitted
θ_w	0.0045	Fitted
Λ_u	1/15	[27]
Λ_v	1/15	[27]
Λ_w	1/15	[27]
ℓ	0.1310	Fitted
ξ	0.3851	Fitted
β	0.1536	Fitted

To fit the model with the cumulative daily reported cases of COVID-19 (which is obtained from the daily reported cases data from August 01 2021 to July 21 2022), we make use of the least squares method with a view to optimize the summation of squared errors defined by $\sum \left(\mathfrak{D}(t,\phi) - \mathfrak{D}_{real}\right)^2$ subject to the COVID-19 model (1), where $\mathfrak{D}_{real}$ is the real cumulated daily reported COVID-19 data, $\mathfrak{D}(t,\phi)$ is the model solution corresponding to the cumulated daily reported cases of COVID-19 data over time t, while ϕ is the target set of estimated parameters. By following the ideas in [24,64], the fitting process is successfully implemented with the use of `fmincon` software package in MATLAB. The values of the demographic parameters ζ and φ along with λ_u are estimated, the values of Λ_u, Λ_v and Λ_w are taken from the established literature, so that the target set of estimated parameters from fitting is $\phi = \{\lambda_u, \lambda_v, \lambda_w, \theta_v, \theta_w, \ell, \xi, \beta\}$.

The average lifespan in India is 69.66 years [15], so that the demographic parameter φ is estimated as $1/(69.66\times365)$ day^{-1}. The total population of India in 2021 was estimated to be 1,393,409,033 [15]. Thus, the total population at initial time $t = 0$ is set at $N(0) = 1\,393\,409\,033$. We further assume that the limiting COVID-19 free total human population is $\zeta/\varphi = 1\,393\,409\,033$, so that $\zeta = 54\,802.74$ day^{-1}. On August 01 2021, the numbers of reported new COVID-19 cases and deaths were 40 134 and 422, respectively. Then, θ_u is estimated as $\theta_u = 422/40134 = 0.0105$ day^{-1}. The recovery period for COVID-19 infection, on average, is around 15 days [27], so that we fix $\Lambda_u = \Lambda_v = \Lambda_w = 1/15$ day^{-1}.

Finally, we obtain the values of the remaining unknown biological parameters by fitting the model to the COVID-19 real data along with the initial conditions estimated as follows: Since there were 40 134 newly reported COVID-19 cases on August 01 2020, we assume that $V(0) = \frac{5}{1000} \times 40134 \approx 201$ and $W(0) = \frac{1}{1000} \times 40134 \approx 40$, so that $U(0) = 40134 - (V(0) + W(0)) = 39\,893$. The number of exposed individuals is assumed to be 20 times that of symptomatic infected individuals, so that $E(0) = 20 \times (U(0) + V(0) + W(0)) = 802\,680$. On this particular date, there were 36,808 and 422 recoveries and deaths, respectively, so we set $R(0) = 36\,808$ and $D(0) = 422$. It is straightforward to obtain the susceptible population at time $t = 0$ as $S(0) = N(0) - (E(0) + U(0) + V(0) + W(0) + R(0) + D(0)) = 1\,392\,528\,989$.

The estimated parameter values obtained from the fitting process are displayed in Table 1. For the COVID-19 outbreaks with the estimated parameter values given in Table 1, the estimated value of the control reproduction number, $\mathcal{R}_0$, is approximately $\mathcal{R}_0 = 1.083$.

Fig. 2 provides the comparison of the actual data and the model's prediction for the number of COVID-19-infected patients in India with the corresponding residuals distribution. Fig. 2(b) shows that residuals are randomly distributed. In this manner, it is sound to say that

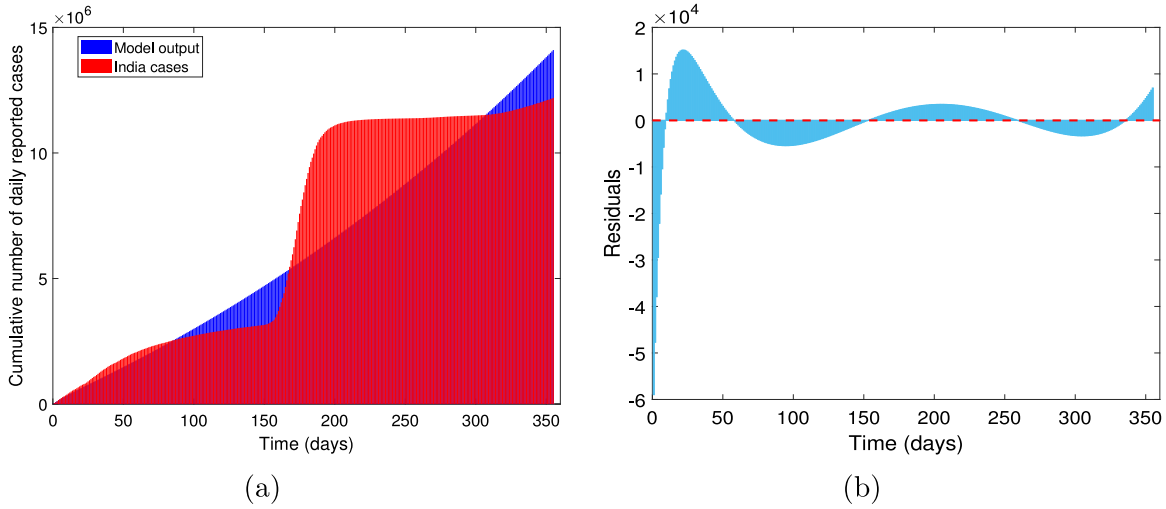

Fig. 2. (a) A graphical comparison of India COVID-19 case data and model prediction between 01 August 2021 and 21 July 2022, (b) Distribution of the residuals of the model simulation.

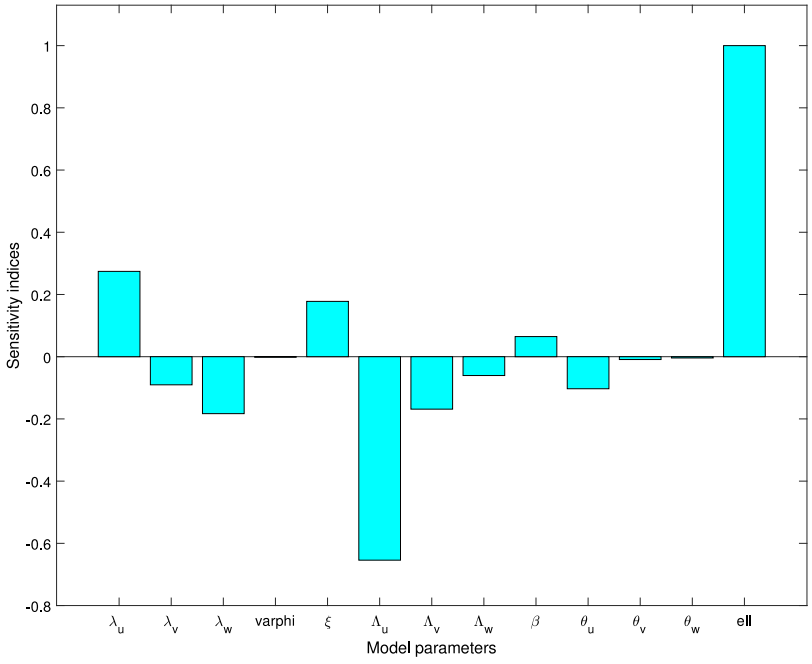

Fig. 3. Sensitivity indexes of $\mathcal{R}_0$ with respect to the parameters defining it.

the estimates obtained from the fitting process are reasonable. These illustrations make it clear to the reader that mathematical models offer a lot of potentials when it comes to articulating challenges that are encountered in the real world. In computing approximations for mathematical models of infectious illnesses, the CFD operator is very trustworthy and efficient.

In Fig. 3, the numerical values of the sensitivity indexes of the reproduction number, $\mathcal{R}_0$, to the parameters defining it are graphically shown.

Fig. 4 shows the behaviours of susceptible people $S(t)$ and exposed people $E(t)$ versus time t in days with variation in the memory index μ at different values of 0.7, 0.8, 0.9 and 1.

In Fig. 5, the behaviours of infected people who did not receive any vaccine $U(t)$, infected people who received the first dose of vaccine $V(t)$ and infected people who received the second (full) dose of vaccine $W(t)$ versus time t in days with variation in the memory index μ at different values of 0.7, 0.8, 0.9 and 1 are illustrated.

In addition, Fig. 6 displays the behaviours of recovered people $R(t)$, and dead people $D(t)$ versus time t in days with variation in the memory index μ at different values of 0.7, 0.8, 0.9 and 1.

Also, we demonstrate the results obtained from the simulations of the COVID-19 model with classical derivative graphically. Fig. 7(a) compares populations with symptoms of infection who have not had any vaccination, those who have received their first dosage, and those who have received their second dose (full) of vaccination. A red line shows populations that have not gotten any vaccinations. Dashed black and continuous blue lines represent the populations that have had their first and second doses of the vaccine, respectively. Similarly, Fig. 7(b) depicts the comparison of the dynamics of recovered and dead individuals. A red line shows people being recovered, and dashed black lines represent the dead people.

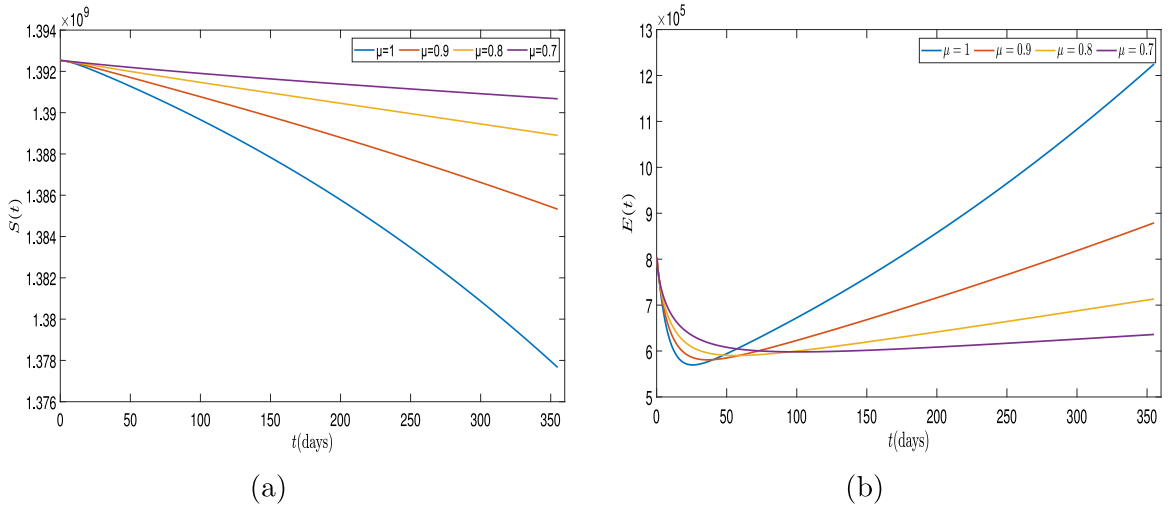

Fig. 4. Dynamical behaviour of (a) susceptible population, (b) exposed population in India for different μ values from 01 August 2021 to 21 July 2022.

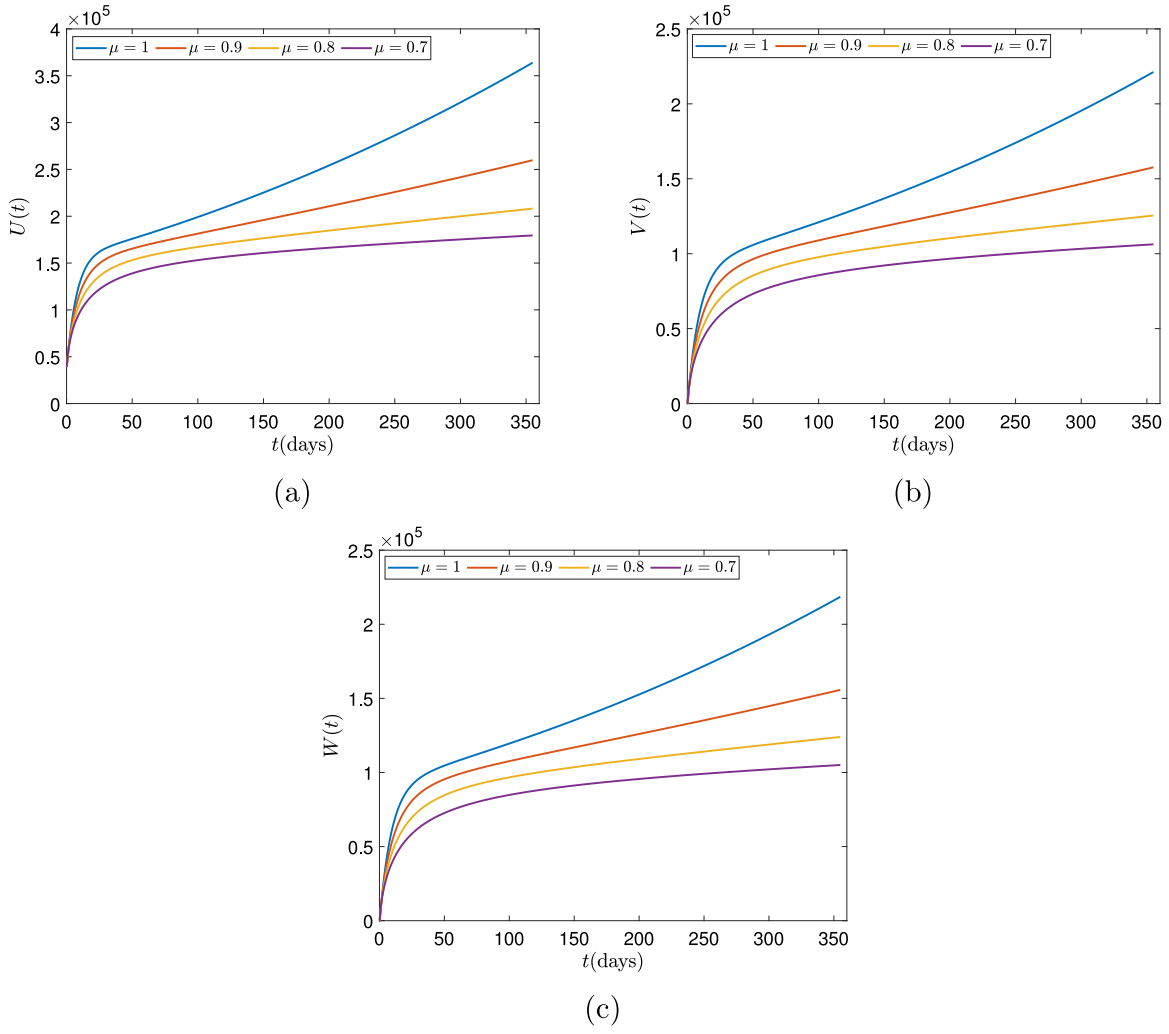

Fig. 5. Dynamical behaviour of symptomatic infected population (a) without vaccination, (b) after the first dose vaccination, (c) after the second dose (full) vaccination for different μ values from 01 August 2021 to 21 July 2022 in India.

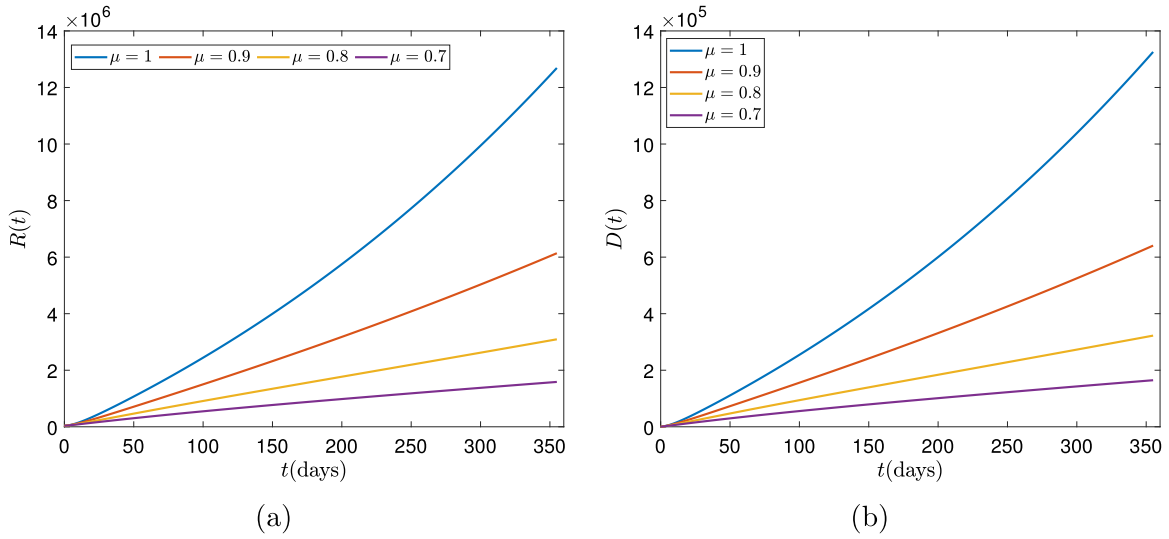

Fig. 6. Dynamical behaviour of (a) recovered population, (b) dead population in India for different μ values from 01 August 2021 to 21 July 2022.

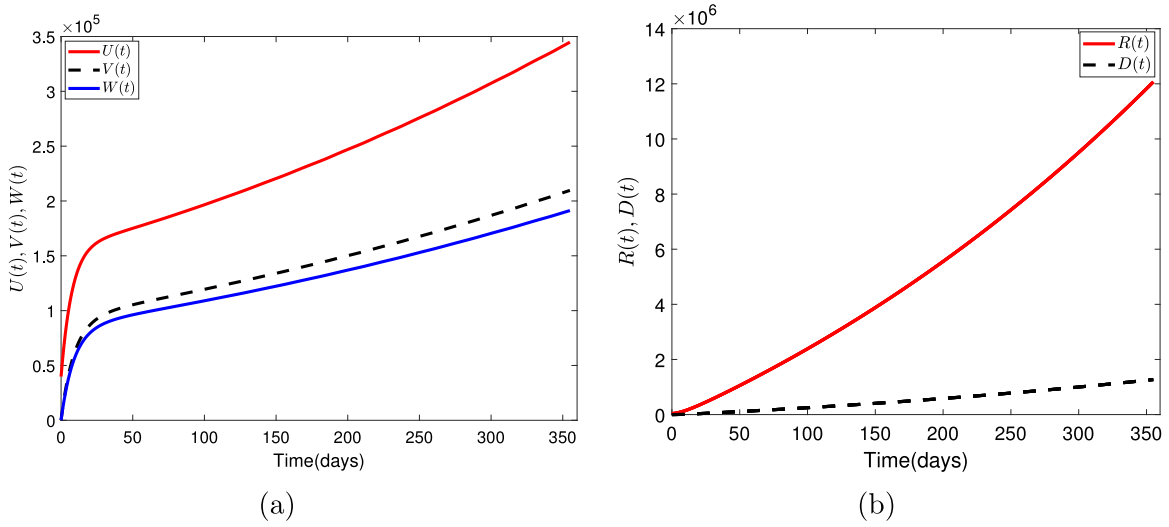

Fig. 7. Time series for (a) various infected populations, (b) recovered and dead populations using the classical derivative and estimated parametric values from 01 August 2021 to 21 July 2022. (For interpretation of the references to colour in this figure legend, the reader is referred to the web version of this article.)

7. Discussion

In the present section, we discuss the results arising from the numerical experiment carried out on the classical and fractional-order COVID-19 models under Section 6.

From Fig. 3, it is observed that of all the positive indices, the effective contact rate, ℓ has the highest. Therefore, ℓ is regarded the most sensitive parameter from the set of parameters with positive index. For example, the computed result $\mathcal{S}_{\ell}^{\mathcal{R}_0} = +1$ suggests that an increase (or decrease) of the value of ℓ by 100% will increase (or decrease) $\mathcal{R}_0$ by 100%. However, the recovery rate of the symptomatic infected people without taking any vaccine, Λ_u, is considered the most sensitive parameter of all the parameters with negative sensitivity indexes shown in Fig. 3 because it has the highest index value. In particular, the result $\mathcal{S}_{\Lambda_u}^{\mathcal{R}_0} = -0.6541$ means that due to an increase (or decrease) of the recovery rate of the symptomatically infected people without taking any vaccine by 10%, the basic reproduction number $\mathcal{R}_0$ of the Caputo fractional order COVID-19 model (6) will decrease (or increase) by 6.541%. Consequently, the sensitivity analysis of model (6) provides useful information about the transmission dynamics of COVID-19 in India.

Fig. 4(a) shows that when the value of μ declines, the number of susceptible people drops fast and converges to zero. The graph in Fig. 4(b) for exposed persons demonstrates that when the value of μ decreases, so does the growth rate of the exposed compartment. Fig. 5(a) indicates that the symptomatic infected population grows rapidly with non-integer values of μ, but the infection rate decreases as the value of μ decreases. It also demonstrates that the number of infected people is much smaller at a faster rate ($\mu = 0.7$). The number of symptomatic infected people after the first dose vaccination and complete vaccination also increases for different values of μ, as depicted in Figs. 5(b) and 5(c), respectively. Similarly, a change in μ causes individuals to recover relatively quickly, as seen in Fig. 6(a). Finally, Fig. 6(b) illustrates people in the dead class, which decreases with fractional values of μ.

Fig. 7(a) demonstrates that after getting both doses of the vaccination, the number of infected persons was much lower than the number of infected people who had not received the vaccine. It is shown that a direct relationship exists between the recovered and dead compartments as seen in Fig. 7(b). In other words, the number of deaths increases as the number of recoveries increases, following the increased number of infected individuals in the population.

7.1. Current situation

The first case of COVID-19 was reported in India on 30 January 2020 [44]. As of 1 June 2022, India had reported a total of $43,847,065$ confirmed cases, with 525,930 deaths. By 16 December 2022, the total number of cases was $44,675,609$, including $44,141,255$ recoveries and 530,663 deaths [65].

7.2. Challenging issues

The greatest challenge in defeating the ongoing COVID-19 pandemic is understanding its complex dynamics. COVID-19 virus evolves as changes in its genetic code occur during replication of the genome. In the second wave of COVID-19, the Omicron variant was discovered with continuous rise in cases [66]. In July 2022, the Omicron variant of concern was the dominant variant circulating around the world. Specifically, Omicron was the dominant variant with 97.6%, and BA.2 being the major sub lineage with 40.8% percent In India [67]. To effectively control the pandemic, vaccine is a highly effective intervention which can considerably reduce the number of infections in the population. A number of vaccines are available for COVID-19, but how these vaccines can be helpful to eradicate the disease is still unknown [66]. Researchers suggest that vaccines are slightly less effective against most of the variants, which may lead to a free spread of the variance [53]. Thus, appropriate and timely application of precautionary measures can essentially diminish the number of newly infected cases globally.

7.3. Government policies proposed

Since the first case of COVID-19 was reported in India, the Indian government has been concerned with the implementation of high measures to lower the rate of disease spread. One of the approach taken by the government during the pre-vaccination regime was to restrict population movements. On 22 March 2020, India observed a day-long countrywide public curfew. Moreover, the government has imposed 21 days nationwide lockdown, counting from 25 March 2020 [44]. A number of other non-pharmaceutical measures were put in place. These include banning travel, closing schools and workplaces, limiting the size of gatherings, maintain social distancing, wearing of face masks in public, and washing hands regularly [55]. To additionally help in relieving the spread of COVID-19 in the country, contact tracing of suspected contaminated cases was stepped up and detected cases are immediately positioned in isolation for treatment [53,55]. It has been observed that people who strictly adhere to precautionary measures are occasionally infected [53]. Interestingly, COVID-19 vaccines became available in the country in January 2021, and the government commenced mass administration of vaccine during the month [13]. As of 16 December 2022, $2,199,939,635$ people have received at least first dose of vaccine [65]. However, combining vaccination strategy with non-pharmaceutical measures has been helpful in the course of fighting against the community spread of COVID-19 pandemic in India, and at global level.

7.4. Future prospects offered

In actual sense, the incidence rates of COVID-19 have been reduced since the commencement of vaccine administration in different countries around the world. In particular, India has witnessed a considerable reduction in the incidence rates of the pandemic dated back to 16 January 2021 when mass vaccine administration commenced in the country. However, this level of infections in the country can be attributed to the combined efforts of vaccine with some public awareness, prevention and treatment roles which the individuals and government health workers have been applied.

Thus, to ensure the protection of the population, our study proposes integer-order and fractional-order deterministic models with unvaccinated, first dose-vaccinated and second dose-vaccinated infected individuals. As observed from the sensitivity analysis, to adequately reduce the community spread of COVID-19, it is vital to reduce the transmission probability per contact, ℓ, and increase the rate of recovery of the unvaccinated infected persons Λ_u. Therefore, despite the huge success of vaccination intervention in COVID-19 control, the efforts of mass vaccination need to be continuously enhanced by personal protection and case management control in order to considerably reduce the susceptibility of the vaccinated individuals to re-infection and the disease prevalence in the population.

8. Conclusions

In this paper, a mathematical model was devised and examined to better explain the dynamics of COVID-19 pandemic following vaccination in India. The equilibrium point for the stated model has been calculated. The basic reproduction number related to the model is also estimated using the next generation matrix technique. To aid the results of theoretical model analysis, numerical simulations are performed. The model is also trained using real-life data to predict cases of infected populations in India as a case study. The results of the proposed model match the real data very closely. This paper also examined the key parameters that influence the dynamics of COVID-19 in the population via a sensitivity analysis. It is shown that effective transmission rate and the recovery rate of unvaccinated infected individuals are the most sensitive parameters. Thus, for the disease control, reducing the virus transmission and improving on the treatment regime for quick recovery of the infected individuals in the population are critical, which can be achieved by increasing the effort of vaccine uptake, ensure strict adherence to self-protective measures, and provision of timely treatment support for the infected people. Numerical simulations reveals that the increase or decrease in the sizes of various epidemiological classes vary at different memory index, and thereby implying that our proposed fractional-order model in Caputo sense is helpful in better understanding of the physical behaviour of COVID-19 transmission and spread in a community. The study recommends that the Indian government should take the necessary steps geared towards reducing the basic reproduction number, $\mathcal{R}_0$, through the sensitive parameters.

It is worth mentioning that the compartmental models studied in this paper are governed by autonomous systems of integer- and fractional-order deterministic models. Also, a successful control strategy which minimizes the numbers of COVID-19 infections and the disease related deaths at the least possible cost is desirable by the government, policy makers and health practitioners. Therefore, in line with the results of the sensitivity analysis obtained in this study, it is worthy to derive the intervention strategy required for an effective control of COVID-19 in the population using the control measures such as optimal personal protection and treatment at possible low cost by formulating an appropriate optimal control framework for the Caputo fractional-order model of COVID-19 dynamics.

Declaration of competing interest

The authors declare that they have no known competing financial interests or personal relationships that could have appeared to influence the work reported in this paper.

Data availability

This manuscript has associated data in a data repository available at Our World in Data

Acknowledgements

Authors would like to express their sincere appreciation to the handling editor and the reviewers for their constructive suggestions that led to the presentation of this improved manuscript. The authors also acknowledged, with gratitude, the funding support from CSIR, MHRD, Government of India, New Delhi, through the grant number (09/843(0006)/2020-EMR-I).

References

[1] H. Zhu, L. Wei, P. Niu, The novel coronavirus outbreak in Wuhan, China, Global Health Res. Policy 5 (1) (2020) 1–3.
[2] Centers for Disease Control and Prevention, Outbreak of 2019 novel coronavirus (2019-nCoV) in Wuhan, China, 2020, www.cdc.gov/csels/dls/locs. Accessed January 21 2020.
[3] World Health Organization, WHO characterizes Covid-19 as a pandemic, 2020, https://www.who.int/emergencies/diseases/novel-coronavirus-2019/situation-reports. Accessed March 11 2020.
[4] U. S. Centers for Disease Control and Prevention (CDC), Coronavirus Disease 2019 (COVID-19): Prevention and Treat- ment, Archived from the original on March 11, 2020, 2020, https://www.who.int/emergencies/diseases/novel-coronavirus-2019/situation-reports. Retrieved March 11, 2020.
[5] World Health Organization, "Advice for Public.," Archived from the original on 26 January 2020, 2020, Retrieved February 10 2020.
[6] S.E. Moore, E. Okyere, Controlling the transmission dynamics of COVID-19, 2020, arXiv preprint arXiv:2004.00443.
[7] S. Mwalili, M. Kimathi, V. Ojiambo, D. Gathungu, R. Mbogo, SEIR model for COVID-19 dynamics incorporating the environment and social distancing, BMC Res. Notes 13 (1) (2020) 1–5.
[8] Kerala defeats coronavirus; India's three COVID-19 patients successfully re-cover, The Weather Channel. Archived from the original on 18 February 2020, 2020, https://www.ncbi.nlm.nih.gov/pmc/articles/PMC7802861/#ref1. Retrieved February 21 2020.
[9] R. Rappuoli, C.W. Mandl, S. Black, E. De Gregorio, Vaccines for the twenty-first century society, Nat. Rev. Immunol. 11 (12) (2011) 865–872.
[10] S. Moore, E.M. Hill, L. Dyson, M.J. Tildesley, M.J. Keeling, Modelling optimal vaccination strategy for SARS-CoV-2 in the UK, PLoS Comput. Biol. 17 (5) (2021) e1008849.
[11] K.D. Elgert, Immunology: Understanding the Immune System, John Wiley & Sons, 2009.
[12] M. Fudolig, R. Howard, The local stability of a modified multi-strain SIR model for emerging viral strains, PLoS One 15 (12) (2020) e0243408.
[13] World Health Organization, India rolled out the world's largest vaccination drive, 2021, https://www.who.int/india/news/feature-stories/detail/india-rolls-out-the-world-s-largest-covid-19-vaccination-drive. Retrieved January 16 2021.
[14] World Health Organization, Second dose is inadvertently administered, 2022, https://www.who.int/news-room/feature-stories/detail/the-bharat-biotech-bbv152-covaxin-vaccine-against-covid-19-what-you-need-to-know. Retrieved June 10 2022.
[15] Our World in Data, Data on COVID-19 (coronavirus), 2022, https://github.com/owid/covid-19-data/tree/master/public/data. Accessed June 10 2022.
[16] A.E. Owoyemi, I.M. Sulaiman, P. Kumar, V. Govindaraj, M. Mamat, Some novel mathematical analysis on the fractional-order 2019-nCoV dynamical model, Math. Methods Appl. Sci. (2022).
[17] M.A. Khan, A. Atangana, Modeling the dynamics of novel coronavirus (2019-nCov) with fractional derivative, Alex. Eng. J. 59 (4) (2020) 2379–2389.
[18] A. Abidemi, K.M. Owolabi, E. Pindza, Modelling the transmission dynamics of Lassa fever with nonlinear incidence rate and vertical transmission, Physica A 597 (2022) 127259.
[19] S. Rezapour, S. Etemad, M. Sinan, J. Alzabut, A. Vinodkumar, A mathematical analysis on the new fractal-fractional model of second-hand smokers via the power law type kernel: Numerical solutions, equilibrium points, and sensitivity analysis, J. Funct. Spaces 2022 (2022).
[20] P. Liu, T. Munir, T. Cui, A. Din, P. Wu, Mathematical assessment of the dynamics of the tobacco smoking model: An application of fractional theory, AIMS Math. 7 (4) (2022) 7143–7165.
[21] A. Abidemi, Optimal cost-effective control of drug abuse by students: insight from mathematical modeling, in: Modeling Earth Systems and Environment, Springer, 2022, pp. 1–19.
[22] A. Abidemi, J. Akanni, Dynamics of illicit drug use and banditry population with optimal control strategies and cost-effectiveness analysis, Comput. Appl. Math. 41 (1) (2022) 1–37.
[23] A.M. Mishra, S.D. Purohit, K.M. Owolabi, Y.D. Sharma, A nonlinear epidemiological model considering asymptotic and quarantine classes for SARS CoV-2 virus, Chaos Solitons Fractals 138 (2020) 109953.
[24] A. Abidemi, Z.M. Zainuddin, N.A.B. Aziz, Impact of control interventions on COVID-19 population dynamics in Malaysia: a mathematical study, Eur. Phys. J. Plus 136 (2021) 237.
[25] A. Džiugys, M. Bieliūnas, G. Skarbalius, E. Misiulis, R. Navakas, Simplified model of Covid-19 epidemic prognosis under quarantine and estimation of quarantine effectiveness, Chaos Solitons Fractals 140 (2020) 110162.
[26] R. ud Din, A.R. Seadawy, K. Shah, A. Ullah, D. Baleanu, Study of global dynamics of COVID-19 via a new mathematical model, Results Phys. 19 (2020) 103468.
[27] D. Okuonghae, A. Omame, Analysis of a mathematical model for COVID-19 population dynamics in Lagos, Nigeria, Chaos Solitons Fractals 139 (2020) 110032.
[28] S.K. Biswas, J.K. Ghosh, S. Sarkar, U. Ghosh, COVID-19 pandemic in India: a mathematical model study, Nonlinear Dynam. 102 (1) (2020) 537–553.
[29] E. Bonyah, S. Ogunlade, S.D. Purohit, J. Singh, Modelling cultural hereditary transmission: Insight through optimal control, Ecol. Complex. 45 (2021) 100890.
[30] H. Habenom, D.L. Suthar, D. Baleanu, S.D. Purohit, A numerical simulation on the effect of vaccination and treatments for the fractional hepatitis b model, J. Comput. Nonlinear Dyn. 16 (1) 011004.
[31] A. Mulualem, S.D. Purohit, P. Agarwal, D.L. Suthar, Atangana–Baleanu derivative-based fractional model of COVID-19 dynamics in Ethiopia, Appl. Math. Sci. Eng. (AMSE) 30 (1) (2022) 634–659.
[32] S. Kumawat, S. Bhatter, D.L. Suthar, S.D. Purohit, K. Jangid, Numerical modeling on age-based study of coronavirus transmission, Appl. Math. Sci. Eng. (AMSE) 30 (1) (2022) 1–26.
[33] J.K.K. Asamoah, E. Okyere, E. Yankson, A.A. Opoku, A. Adom-Konadu, E. Acheampong, Y.D. Arthur, Non-fractional and fractional mathematical analysis and simulations for Q fever, Chaos Solitons Fractals 156 (2022) 111821.
[34] A. Zeb, A. Atangana, Z.A. Khan, S. Djillali, A robust study of a piecewise fractional order COVID-19 mathematical model, Alex. Eng. J. 61 (7) (2022) 5649–5665.
[35] P.A. Naik, K.M. Owolabi, M. Yavuz, J. Zu, Chaotic dynamics of fractional order HIV-1 model involving AIDS-related cancer cells, Chaos Solitons Fractals 140 (2020) 110272.
[36] P.A. Naik, J. Zu, K.M. Owolabi, Global dynamics of a fractional order model for the transmission of HIV epidemic with optimal control, Chaos Solitons Fractals 138 (2020) 109826.
[37] O.J. Peter, A. Yusuf, M.M. Ojo, S. Kumar, N. Kumari, F.A. Oguntolu, A mathematical model analysis of meningitis with treatment and vaccination in fractional derivatives, Int. J. Appl. Comput. Math. 8 (3) (2022) 1–28.
[38] A. Atangana, Modelling the spread of COVID-19 with new fractal-fractional operators: can the lockdown save mankind before vaccination? Chaos Solitons Fractals 136 (2020) 109860.
[39] N. Sweilam, S. Al-Mekhlafi, S. Shatta, D. Baleanu, Numerical treatments for the optimal control of two types variable-order COVID-19 model, Results Phys. (2022) 105964.
[40] S. Boccaletti, W. Ditto, G. Mindlin, A. Atangana, Modeling and forecasting of epidemic spreading: The case of Covid-19 and beyond, Chaos Solitons Fractals 135 (2020) 109794.
[41] P.A. Naik, K.M. Owolabi, J. Zu, M. Naik, Modeling the transmission dynamics of COVID-19 pandemic in Caputo type fractional derivative, J. Multiscale Model. 12 (3) (2021) 2150006.
[42] H. Habenom, M. Aychluh, D.L. Suthar, Q. Al-Mdallal, S.D. Purohit, Modeling and analysis on the transmission of covid-19 Pandemic in Ethiopia, Alex. Eng. J. 61 (7) (2022) 5323–5342.
[43] F. Nabizadeh, E. Ramezannezhad, K. Kazemzadeh, E. Khalili, E.M. Ghaffary, O. Mirmosayyeb, Multiple sclerosis relapse after COVID-19 vaccination: a case report-based systematic review, J. Clin. Neurosci. 124 (2022) 118–125.
[44] A.S. Shaikh, I.N. Shaikh, K.S. Nisar, A mathematical model of COVID-19 using fractional derivative: outbreak in India with dynamics of transmission and control, Adv. Difference Equ. 2020 (1) (2020) 1–19.
[45] C. Chakraborty, G. Agoramoorthy, India's cost-effective COVID-19 vaccine development initiatives, Vaccine 38 (50) (2020) 7883.
[46] K.G.M. Danabal, S.S. Magesh, S. Saravanan, V. Gopichandran, Attitude towards COVID 19 vaccines and vaccine hesitancy in urban and rural communities in Tamil Nadu, India–a community based survey, BMC Health Serv. Res. 21 (1) (2021) 1–10.
[47] S. Bagcchi, The world's largest COVID-19 vaccination campaign, Lancet Infect. Dis. 21 (3) (2021) 323.
[48] B.H. Foy, B. Wahl, K. Mehta, A. Shet, G.I. Menon, C. Britto, Comparing COVID-19 vaccine allocation strategies in India: A mathematical modelling study, Int. J. Infect. Dis. 103 (2021) 431–438.
[49] O. Okundalaye, W. Othman, A. Oke, Toward an efficient approximate analytical solution for 4-compartment COVID-19 fractional mathematical model, J. Comput. Appl. Math. 416 (2022) 114506.
[50] P. Agarwal, M.A. Ramadan, A.A. Rageh, A.R. Hadhoud, A fractional-order mathematical model for analyzing the pandemic trend of COVID-19, Math. Methods Appl. Sci. 45 (8) (2022) 4625–4642.
[51] I. Aldawish, R.W. Ibrahim, A new mathematical model of multi-faced COVID-19 formulated by fractional derivative chains, Adv. Contin. Discrete Models 2022 (1) (2022) 1–10.
[52] R.M. Pandey, A. Chandola, R. Agarwal, Mathematical model and interpretation of crowding effects on SARS-CoV-2 using Atangana-Baleanu fractional operator, in: Methods of Mathematical Modelling, Elsevier, 2022, pp. 41–58.

[53] Z. Ali, F. Rabiei, M.M. Rashidi, T. Khodadadi, A fractional-order mathematical model for COVID-19 outbreak with the effect of symptomatic and asymptomatic transmissions, Eur. Phys. J. Plus 137 (3) (2022) 1–20.
[54] A.M. El-Sayed, A. Arafa, A. Hagag, Mathematical model for the novel coronavirus (2019-nCOV) with clinical data using fractional operator, Numer. Methods Partial Differential Equations (2022).
[55] V. Padmapriya, M. Kaliyappan, Fuzzy fractional mathematical model of COVID-19 epidemic, J. Intell. Fuzzy Systems (Preprint) (2022) 1–23.
[56] K.S. Miller, B. Ross, An Introduction to the Fractional Calculus and Fractional Differential Equations, Wiley, New Jersey, U.S., 1993.
[57] Z. Ali, F. Rabiei, K. Shah, T. Khodadadi, Qualitative analysis of fractal-fractional order COVID-19 mathematical model with case study of Wuhan, Alex. Eng. J. 60 (1) (2021) 477–489.
[58] I.N. Sneddon, Fourier Transforms, Courier Corporation, Massachusetts, U.S.A., 1995.
[59] L. Kexue, P. Jigen, Laplace transform and fractional differential equations, Appl. Math. Lett. 24 (12) (2011) 2019–2023.
[60] K.M. Owolabi, E. Pindza, A nonlinear epidemic model for tuberculosis with Caputo operator and fixed point theory, Healthc. Anal. 2 (2022) 100111.
[61] P. van den Driessche, J. Watmough, Reproduction numbers and sub-threshold endemic equilibria for compartmental models of disease transmission, Math. Biosci. 180 (1) (2002) 29–48.
[62] A. Atangana, S.I. Araz, New Numerical Scheme with Newton Polynomial: Theory, Methods, and Applications, Academic Press, Cambridge, Massachusetts, 2021.
[63] G. Nazir, A. Zeb, K. Shah, T. Saeed, R.A. Khan, S.I.U. Khan, Study of COVID-19 mathematical model of fractional order via modified Euler method, Alex. Eng. J. 60 (6) (2021) 5287–5296.
[64] A. Abidemi, N.A.B. Aziz, Analysis of deterministic models for dengue disease transmission dynamics with vaccination perspective in Johor, Malaysia, Int. J. Appl. Comput. Math. 8 (1) (2022) 1–51.
[65] Government of India, IndiaFightsCorona COVID-19, 2022, https://www.mygov.in/covid-19/. Accessed December 16 2022.
[66] M. Farman, M. Amin, A. Akgül, A. Ahmad, M.B. Riaz, S. Ahmad, Fractal fractional operator for COVID-19 (Omicron) variant outbreak with analysis and modeling, Results Phys. (2022) 105630.
[67] World Health Organization. Coronavirus Disease COVID-19 situation update report – 116. https://cdn.who.int/media/docs/default-source/wrindia/situation-report/india-situation-report-116.pdf?sfvrsn=1a5f2a59_2.